SCIENTIFIC REPORTS

OPEN

SUBJECT AREAS:
COMPLEX NETWORKS
NONLINEAR PHENOMENA

Received
18 September 2014

Accepted
6 January 2015

Published
4 February 2015

Correspondence and requests for materials should be addressed to Z.-K.G. (zhongkegao@tju.edu.cn.)

Multi-frequency complex network from time series for uncovering oil-water flow structure

Zhong-Ke Gao[1], Yu-Xuan Yang[1], Peng-Cheng Fang[1], Ning-De Jin[1], Cheng-Yi Xia[2] & Li-Dan Hu[1]

[1]School of Electrical Engineering and Automation, Tianjin University, Tianjin 300072, China, [2]Key Laboratory of Computer Vision and System (Ministry of Education) and Tianjin Key Laboratory of Intelligence Computing and Novel Software Technology, Tianjin University of Technology, Tianjin 300384, China.

Uncovering complex oil-water flow structure represents a challenge in diverse scientific disciplines. This challenge stimulates us to develop a new distributed conductance sensor for measuring local flow signals at different positions and then propose a novel approach based on multi-frequency complex network to uncover the flow structures from experimental multivariate measurements. In particular, based on the Fast Fourier transform, we demonstrate how to derive multi-frequency complex network from multivariate time series. We construct complex networks at different frequencies and then detect community structures. Our results indicate that the community structures faithfully represent the structural features of oil-water flow patterns. Furthermore, we investigate the network statistic at different frequencies for each derived network and find that the frequency clustering coefficient enables to uncover the evolution of flow patterns and yield deep insights into the formation of flow structures. Current results present a first step towards a network visualization of complex flow patterns from a community structure perspective.

The oil-water mixture flow widely exists in oil exploitation and petrochemical industries. The single-phase flow and two-phase flow are very different and the intrinsic difference lies in the occurrence of flow pattern, which is defined by temporal-spatial configuration of the immiscible two phases in a pipe. The study of oil-water flow pattern is crucial for oil industrial processes, e.g., the artificial lift methods in oil wells and flow equipments design all depend on the flow patterns. Horizontal oil-water flow pattern presents stratified structural features at low flow rate; with the increase of flow rate, the structural features of stratified with interfacial waves occurs; At a high flow rate, flow pattern exhibits dispersed flow structure.

The investigation of experimental oil-water flows is a foundational issue of significant importance and it has drawn much attention from chemical engineering and physical research areas. The experimental observation[1], numerical simulation[2], support vector machine[3], particle image velocimetry technique[4], multivariate recurrence networks[5], wavelet multiresolution technique[6] and measurement techniques based on wire-mesh sensor[7], optical probes[8], high frequency impedance probe[9], and parallel-wire capacitance probe[10] have been implemented to the investigation of oil-water flows. Despite the existing results, how to reveal the complex oil-water flow structure from experimental signals still represents a significant challenge. Although the traditional single sensor measurement combined with the approaches for analyzing univariate signals, e.g., the conductance ring sensor combined with fractal analysis, have been successfully introduced into the investigation of gas-liquid flows[11], these analytical frameworks are incapable of revealing the complicated local oil-water flow structures, mainly on account of the existence of physical foundational differences between these two distinct flow situations. Aiming to reveal the oil-water flow structure, we need to use distributed sensors to measure the information of local flow behavior from different positions. Next, how to access to flow structure from the multivariate signals appears as a key challenge. In this regard, developing an efficient approach to realize information fusion and then to uncover the horizontal oil-water flow structures would be particularly helpful and necessary.

Complex network has undergone a remarkable development in the last decade and it provides us a powerful framework for investigating complex systems from different disciplines[12–30]. Representing system components as nodes and regarding the interactions between nodes as edges allows us to infer a complex network from a complex system. For a real complex network, there often exist various community structures: within a community nodes are densely connected while between communities links are sparse. Community detection is of great importance for investigating the function and structure of complex networks. Different methods have been put forward for

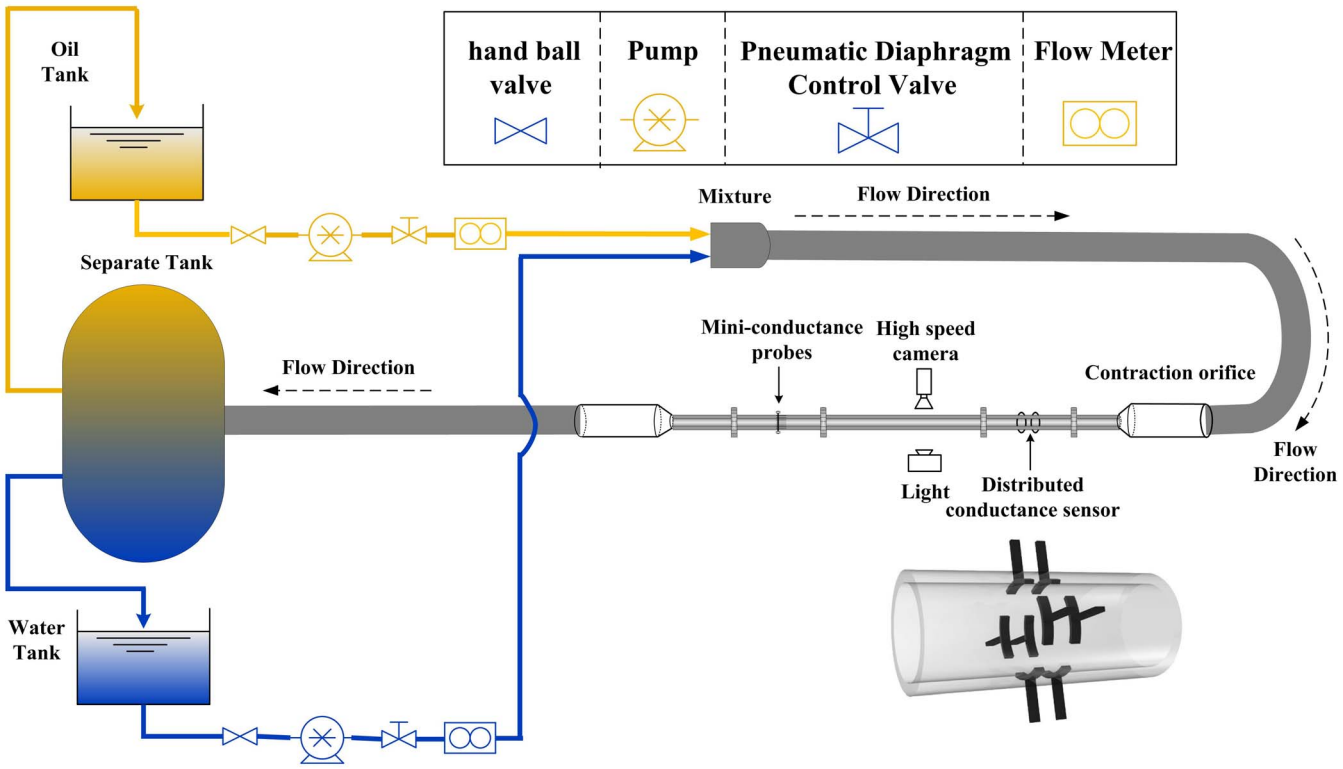

Figure 1 | **Experimental flow loop facility.** The multivariate signals are measured from the distributed conductance sensor. The high speed camera and mini-conductance probes are exploited to define oil-water flow patterns and flow structures.

efficiently detecting network community[31–37]. Quite recently, the complex network theory has greatly contributed to the analysis of time series[38–45], including the research area of climate[46–47], gene[48], brain network[49], grain networks[50], network topology estimation[51], friction networks[52], traffic flow[53], turbulent heated jets[54] and multiphase flow system[55–59], etc. Bridging multivariate data analysis and complex network allows establishing a novel analytical framework for realizing multivariate information fusion.

We previously proposed a multivariate recurrence network to distinguish different horizontal oil-water flow patterns[5] and study dynamical flow behavior underlying oil-water stratified flows[57]. The former network methodologies focus on the phase-space reconstruction and recurrence analysis. As a further study, we in this paper propose a novel approach to derive multi-frequency complex network from multivariate time series and then visualize and uncover the complex flow structure in terms of community structure at different frequencies. In particular, we conduct experiments and use our newly designed distributed conductance sensor to measure local flow signals at different positions for each flow pattern. Then, we derive multi-frequency complex networks from multivariate measurements and detect network communities at different frequencies. The results suggest that the networks community structures faithfully represent the structural features of different oil-water flow patterns. Our analytical framework can be treated as a network visualization of complex flow structures from a community structure perspective. In order to quantitatively assess the characteristics underlying community structures, we investigate the network statistic at different frequencies and find that the frequency clustering coefficient allows us to uncover the formation and evolution of different oil-water flow structures.

Results

Experimental design and data acquisition. The experiment was carried out in the key laboratory of multiphase flow at Tianjin University. Figure 1 shows experimental flow loop facility and our newly designed distributed conductance sensor. The inner-diameter

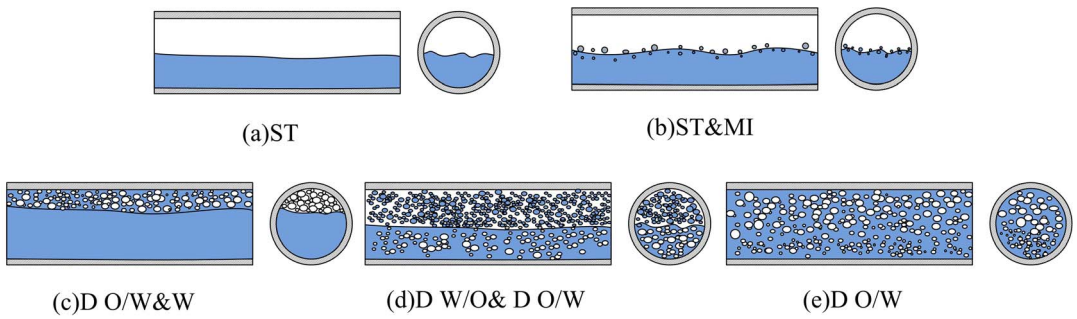

Figure 2 | **Five types of horizontal oil-water flow patterns.** (a) Stratified flow (ST); (b) Stratified flow with mixing at an interface (ST&MI); (c) Dispersion of oil in water and water flow (D O/W&W); (d) Dispersion of water in oil and oil in water flow (D W/O& D O/W); (e) Dispersion of oil in water flow (D O/W).

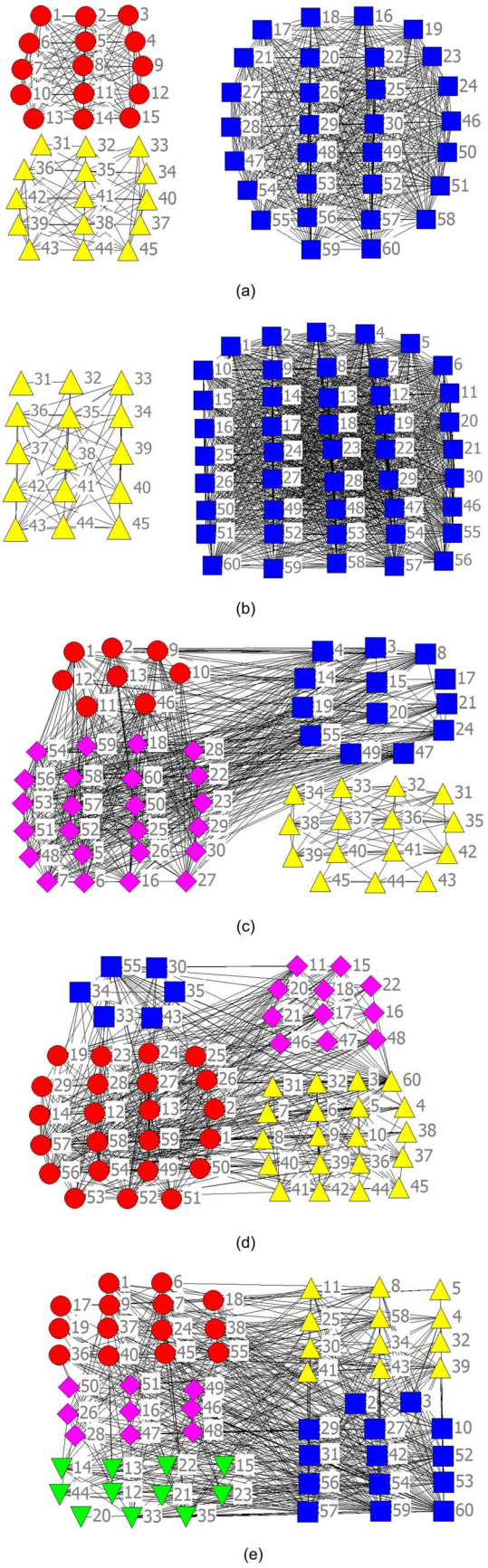

Figure 3 | Community structures of the multi-frequency complex networks for five horizontal oil-water flow patterns. (a) ST; (b) ST&MI; (c) D O/W&W; (d) D W/O& D O/W; (e) D O/W. The networks from different flow patterns exhibit distinct community structures and the community structures faithfully represent the structural features of different flow patterns.

of the horizontal pipe is 20 mm and the media are oil and tap water. The experimental environment temperature and pressure is 25 degrees Celsius and atmospheric pressure, respectively. We first input oil and water mixture into a horizontal pipe at a fixed water flow rate, then gradually change oil flow rate. A flow condition can be obtained each time when the flow rates of oil and water attain a pre-defined ratio, and then we acquire the multivariate signals from our designed distributed conductance sensor. The water flow rate and oil flow rate can be accurately measured by using electromagnetic flow meter and turbine flow meter, respectively. The sampling frequency is 4000 Hz and the measuring time for one measurement is 30 s. We in the experiment generate five typical horizontal oil-water flow structures (flow patterns), as shown in Fig. 2, including ST (stratified flow), ST&MI (stratified flow with mixing at an interface), D O/W&W (dispersion of oil in water & water flow), D W/O& D O/W (dispersion of water in oil & dispersion of oil in water flow), D O/W (dispersion of oil in water flow). The range of Reynold number is 300 ~ 6000. The multivariate signals measured from our distributed sensors consist of four time series, each of which is obtained with a sector sensor that is placed at different positions of the horizontal pipe so as to effectively capture the local flow information.

Network visualization of flow patterns in terms of community structure. Complex networks usually can be divided into communities with a large number of internal connections, interconnected by fewer external edges. The information mined from the detected community structures is of great values, e.g., the community structure of brain network allows revealing the functional connectivity and interaction underlying the complex brain system. Based on the experimental multivariate signals, we use our proposed framework to infer numbers of multi-frequency complex networks for different flow conditions. Then we employ a fast multi-scale community detection algorithm[37] to detect the network communities associated with flow structures at different frequencies. In particular, after inferring networks for the frequency band 0 ~ 30 Hz, we detect the community structures at different frequencies for different flow patterns and find that the modularity of ST, ST&MI, D O/W&W, D W/O& D O/W and D O/W reaches a stable maximum at the frequency band of 0 ~ 20 Hz, 0 ~ 20 Hz, 5 ~ 25 Hz, 5 ~ 25 Hz, 10 ~ 30 Hz, respectively. This result can be well supported by the existing knowledge about the local movement frequencies of different flow patterns. We show the detected network structures of the maximum modularity for different flow patterns in Fig. 3.

For the ST flow structure, oil phase and water phase continuously flow in the upper part and bottom part of the horizontal pipe, respectively. There exists an oil-water interface without the occurrence of droplets, as shown in Fig. 2(a). Correspondingly, the network community structure of ST flow is composed of three communities, as shown in Fig. 3(a). With an increase in oil flow rate under an unchanged water flow rate, large amplitude fluctuations appear and then gradually increase at oil-water interface (Fig. 2(b)), and correspondingly, liquid droplets of different size occur near the oil-water interface and the thickness of oil layer becomes thicker, reflecting the flow structure of the ST&MI flow pattern. Consequently, the network community structure of ST&MI flow consists of a very big community and a small community, which is different to that of ST flow pattern, as can be seen in Fig. 3(b). For the segregated flows (ST, ST&MI), the separated community that is represented by yellow triangle results from the bottom local flow

structure of water continuous flow, as shown in Fig. 3(a)–(b). D O/W&W flow structure (Fig. 2(c)) presents the features of oil droplets dispersedly flowing in a water continuum in the upper and middle part, and a continuous water layer flowing in the bottom part. Correspondingly, there exist four network communities underlying D O/W&W flow structure, as can be seen from Fig. 3(c), wherein the separated one corresponds to the water layer and the other three result from the flow behavior of dispersed oil droplets. With the increase of the oil flow rate, oil droplets disperse into water continuous phase in the bottom part and the flow structure in upper part evolves into oil containing dispersed water droplets, and flow structure in the middle part is the stochastic movements of numerous dispersed water and oil droplets, i.e., the D W/O&D O/W flow pattern occurs (Fig. 2(d)). Since the flow structure becomes more complicated in the transformation from D O/W&W flow to D W/O&D O/W flow, the community structure of the D W/O&D O/W flow becomes more complex than that of D O/W&W flow, as can be seen from Fig. 3(d), and there are four communities and there does not exist such a separated community shown in Fig. 3(c). The flow structure will evolve into D O/W at a high water flow rate (Fig. 2(e)), in which dispersed oil droplets randomly flowing in water continuum for the whole horizontal pipe, consequently, the dynamic flow behavior and flow structure become very complicated. We can see from Fig. 3(e) that, the community structure of the D O/W flow is similar to that of D W/O&D O/W flow, but there exist five communities, i.e., number of community is more than that of D W/O&D O/W flow. Therefore, based on the multivariate signals from distributed conductance sensor, the community structures of multi-frequency complex networks allow us to recognize different flow patterns and further pave a way for realizing network visualization of complex flow structures. In the next section, we will use a network statistic to quantitatively uncover the flow behavior which accounts for the evolution of flow patterns and formation of flow structures.

Dynamical characterization of flow pattern transitions. Our methodology allows mapping multivariate signals acquired from our distributed sensors into a multi-frequency complex network in the frequency range of 0 ~ 30 Hz. We derive multi-frequency complex networks from experimental measurements for different flow patterns. Then we exploit the network frequency clustering coefficient to quantitatively assess the characteristics of each derived network. The clustering coefficient proposed by Watts et al.[60] measures denseness of connections among the neighbors of a given node, which allows us to access to the local topological connections underlying a complex network. In particular, for our multi-frequency complex network, a clustering coefficient of a node v at frequency f, i.e., $C_v(f)$, can be calculated as follows:

$$C_v(f) = \frac{2E_v(f)}{k_v(f)\cdot(k_v(f)-1)} = \frac{\sum_{j,m} A_{ij}(f)A_{im}(f)A_{mj}(f)}{k_v(f)\cdot(k_v(f)-1)} \quad (1)$$

where $E_v(f)$ is the number of closed triangles containing node v at frequency f and $k_v(f)$ is the degree of the node v at frequency f, which is defined as the number of connections to node v at frequency f. The frequency clustering coefficient for the network at frequency f can then be obtained by

$$C(f) = \frac{1}{N}\sum_{v=1}^{N} C_v(f) \quad (2)$$

where N is the total number of nodes. In our multi-frequency complex network analysis, we focus on the frequency bands within which the modularity is larger than 0.1, and then calculate the frequency clustering coefficients $C(f)$ at these frequency bands and correspondingly calculate the mean value and standard deviation of $C(f)$ for different frequencies (for one flow condition). We in Fig. 4 present mean values $<C(f)>$ and standard deviations (error bars) of $C(f)$for different flow conditions arising from five different flow structures.

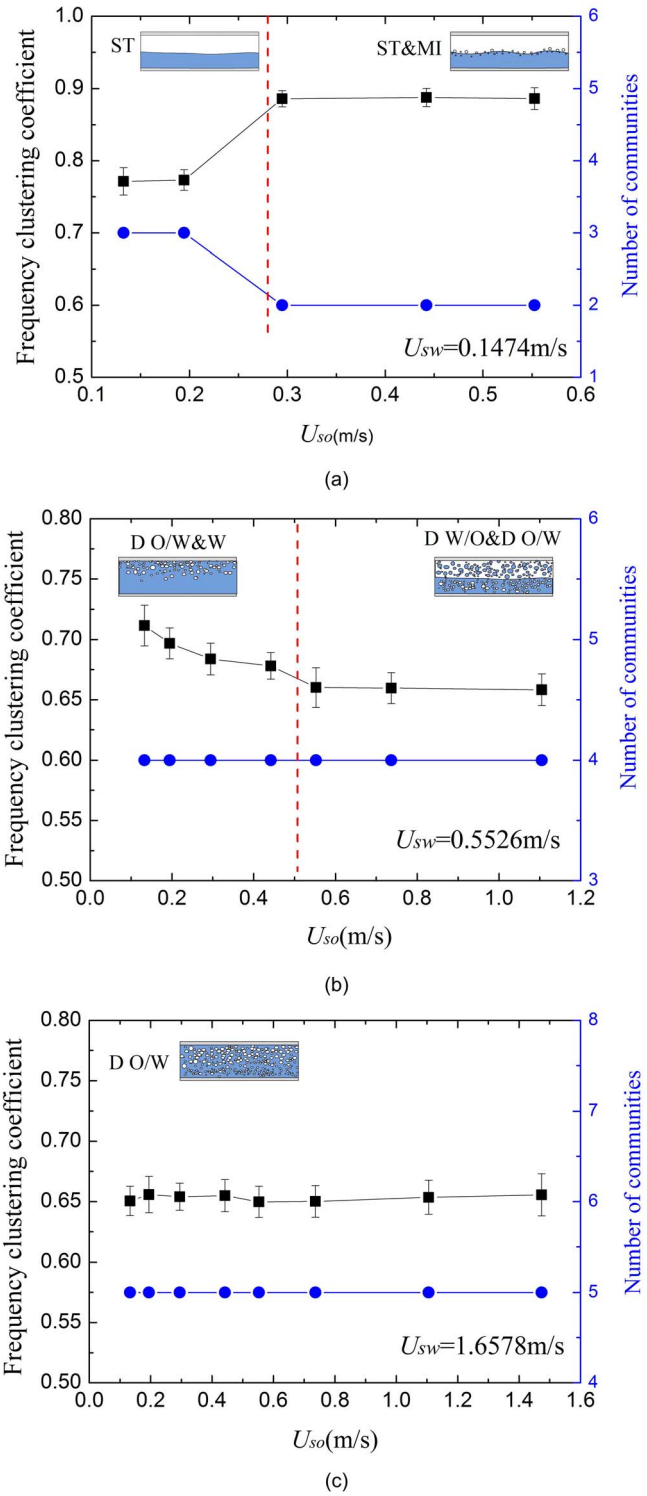

Figure 4 | Distributions of frequency clustering coefficients and number of communities for the transitions of different horizontal oil-water flow patterns. The square symbols represent the distributions of frequency clustering coefficients and the circular symbols represent the number of communities for different flow patterns.

The ST flow and ST&MI flow are sorted into segregated flow, in which the oil phase and water phase locate in the upper and bottom part, respectively, and the two phases are separated. As can be seen, the frequency clustering coefficients for ST flow and ST&MI flow

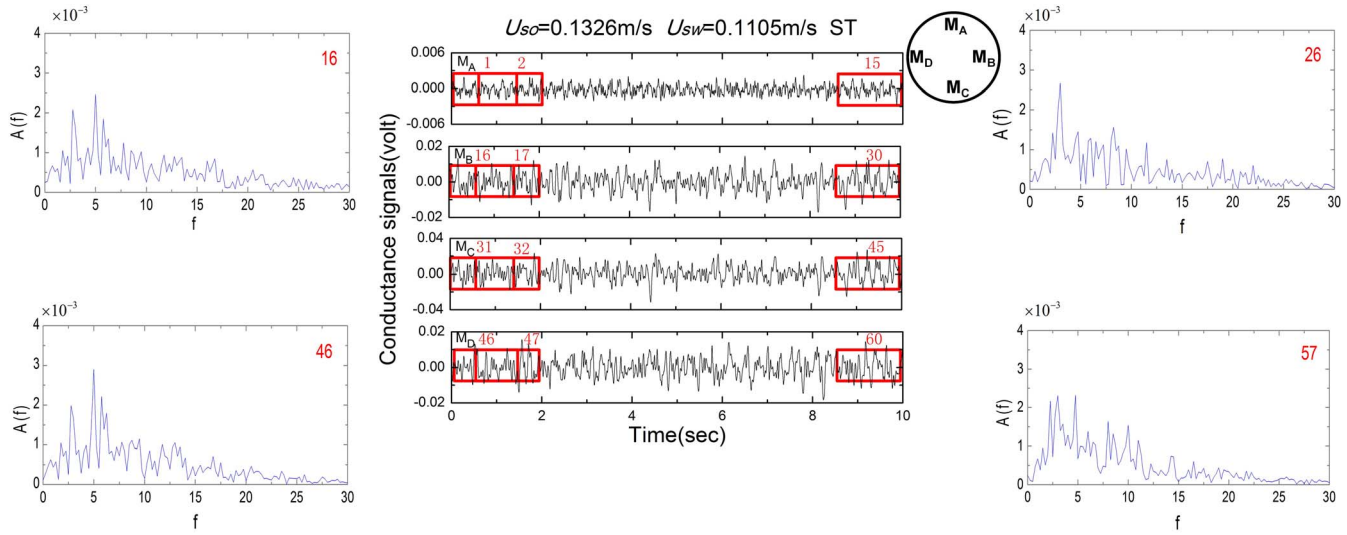

Figure 5 | Schematic diagram for the construction of multi-frequency complex network.

locate in two different regions. A characteristic change of $<C(f)>$ occurs when the flow structure evolves from ST type to ST&MI type. ST flow structure occurs at low water and low oil flow rates, and under these flow conditions the momentum instabilities remain minimal and the gravity plays a dominated role. So the ST flow structure is usually steady and its interfacial wave behavior is not obvious. With an increase in oil flow rate under an unchanged water flow rate, the relative movement between water phase and oil phase increases, which contribute to the appearance and growth of interfacial waves. This is an onset of ST&MI flow structure, in which drag force enhanced by the increased relative movements overcomes the surface tension force, resulting in the deformation of oil-water interfacial wave and formation of liquid droplets. In particular, in ST&MI flow, the hydrodynamics forces the liquid drops to distribute on pipe cross-section, while meantime the buoyancy reacts on the drops to resist the downtrend caused by gravity. By further increasing the flow rate, the interfacial wave propagation is greatly strengthened, and eventually leads to the formation of more liquid drops at oil-water interface. From Fig. 4(a) we can see that, $<C(f)>$ for ST flow are of small values, but with the increase of oil flow rate, e.g., U_{so} = 0.2947 m/s, the $<C(f)>$ will increase from 0.773 to 0.886, indicating interfacial wave behavior becomes enhanced and unstable and at the meantime the liquid droplets are formed at the interface.

Besides the ST and ST&MI flow, the other three flows are classified into dispersed flows. The typical features of dispersed flows lie in the existence of one dispersed phase. D O/W&W flow structure appears at high water flow rates and middle oil flow rates. As the oil flow rate further increases, the density of oil phase increases and the turbulence energy of the mixture flow also increases. Consequently, in the upper part the local flow structure evolves from oil in water form to water in oil form and local flow structure in the bottom part is numerous dispersed oil droplets flowing in water continuum, indicating the occurrence of D W/O&D O/W flow structure. In D W/O&D O/W flow structure, the dispersed water/oil droplets randomly flow in the continuous oil/water phase in the upper/bottom part of the horizontal pipe. Correspondingly, as can be seen from Fig. 4(b), the values of $<C(f)>$ for D O/W&W flow structure are relative large (but smaller than that of ST flow structure and ST&MI flow structure), and it decreases in the transition to D W/O&D O/W flow structure, indicating the stochastic flow of plenty of oil drops induced by the increase of oil flow rate. When the water flow rate is very high, the D O/W flow pattern occurs, in which the cross-sectional area of the pipe is occupied by water containing dispersed oil droplets. The dynamic behaviors underlying the motions of massive dispersed oil droplets are rather stochastic. Correspondingly, the $<C(f)>$ for D O/W flow structure is rather small (Fig. 4(c)), which is similar to that of D W/O&D O/W flow but different to other flow patterns. Therefore, the frequency clustering coefficient from multi-frequency complex network enables to efficiently characterize the evolution of oil-water flow structures. For instance, when an evolution in oil-water flow structure occurs, a characteristic change in $<C(f)>$ arises. In addition, we can see that, the values of $<C(f)>$ for different flow structures are distinct, except for D W/O&D O/W flow and D O/W flow. But the number of communities (community structure) for D W/O&D O/W flow structure and D O/W flow structure is different, which provides complementary information for the frequency clustering coefficient. Combining the frequency clustering coefficient and the number of communities provide us a reference frame for recognizing flow structures and characterizing flow behavior. All these findings suggest that the analytical framework of multi-frequency complex network is an efficacious and intuitionistic method for uncovering complex oil-water flow structures.

Discussions

The investigation of complex oil-water flow structures is a fundamental issue eliciting a great deal of interest and attention from different research fields. We have proposed a framework of multi-frequency complex network to visualize horizontal oil-water flow structures and then investigated the evolution of different flow structures from experimental multivariate signals. The basic idea is to construct multi-frequency complex network from experimental multivariate measurements and then to detect the network communities associated with flow structures and finally to extract network statistic at different frequencies for quantitatively uncovering the flow characteristics in the evolution of flow patterns. Our findings indicate that the community structures faithfully represent the structural features of different flow patterns and the frequency clustering coefficients cast light on the local flow behaviors governing the formation and transition of flow structures. Our analytical framework paves the way towards the network visualization of complex flow structures arising from multiphase flow, and also establishes a novel method for analyzing multivariate time series.

Methods

Multi-frequency complex network from multivariate time series. The construction of multi-frequency complex network is based on the Fast Fourier transform (FFT), which allows computing the discrete Fourier transform (DFT) in a much faster way. It is obtained by decomposing a series of values into components of different frequencies as follows:

$$X(f)=\sum_{n=0}^{N-1}x(n)e^{-i\frac{2\pi}{N}nf} \quad (3)$$

where f is the frequency and $X(f)$ is the spectrum value. We now start with the construction of multi-frequency complex network. For a multivariate time series, e.g., the experimental signals M_A, M_B, M_C, M_D measured from our distributed conductance sensor, we first partition each time series into 15 segments with an equal length of 16000. As shown in Fig. 5, for one time series, the segment slides with the time from left to right by a step of 6000. By this operation we can obtain totally 60 segments from our four experimental signals. Then we perform the fast Fourier transform on the 60 segments to obtain the corresponding 60 frequency spectrums by equation (3). The results indicate that the frequency spectrums of the segments from our experimental signals mainly focus on $0 \sim 30$ Hz, as shown in Fig. 5. We denote the mean value of spectrum for $0 \sim 1$ Hz, $1 \sim 2$ Hz, …, $29 \sim 30$ Hz of segment i as $X_i(1), X_i(2), \ldots, X_i(30)$, respectively, $i = 1,2,\ldots,60$. Thus we can obtain $X_i(f), f = 1 \sim 30$, $i = 1 \sim 60$, where f is the frequency and i is the label of segment. Finally, for a certain frequency f, we infer complex network by regarding $X_i(f)$ ($i = 1 \sim 60$) as a node and determining a connection between node i and j by

$$d_{ij}(f)=\left|X_i(f)-X_j(f)\right|,\ 1\le i\ne j\le 60 \quad (4)$$

Specifically, for an unweighted network, we need to select a threshold to determine whether there exists an edge between two nodes. Here we realize this and then obtain an adjacency matrix for a network at frequency f as follows:

$$A_{ij}(f)=\begin{cases}1, & if \quad d_{ij}(f)\le\varepsilon\cdot\max\limits_{1\le i\ne j\le 60}\left|X_i(f)-X_j(f)\right|\\ 0, & if \quad d_{ij}(f)>\varepsilon\cdot\max\limits_{1\le i\ne j\le 60}\left|X_i(f)-X_j(f)\right|\end{cases} \quad (5)$$

Note that the parameter ε here is chosen to make the constructed network have a high and steady-state modularity value in the sense that we expect to arrive at a reliable result of network communities associated with flow structures. The modularity can be evaluated by

$$Q=\sum_i(e_{ii}-a_i^2) \quad (6)$$

where e_{ij} is the fraction of edges that connect nodes within community i to the nodes within community j, $a_i = \Sigma_j e_{ij}$. Therefore, the above framework allows us to derive a series of complex networks at different frequencies, i.e., multi-frequency complex network, from multivariate time series.

1. Trallero, J.-L., Sarica, C. & Brill, J.-P. A study of oil-water flow patterns in horizontal pipes. *SPE Production & Facilities* **12**, 165–172 (1997).
2. Ng, T.-S., Lawrence, C.-J. & Hewitt, G.-F. Interface shapes for two-phase laminar stratified flow in a circular pipe. *Int. J. Multiphase Flow* **27**, 1301–1311 (2001).
3. Ye, J. & Guo, L.-J. Multiphase flow pattern recognition in pipeline-riser system by statistical feature clustering of pressure fluctuations. *Chem. Eng. Sci.* **102**, 486–501 (2013).
4. Morgan, R. G., Markides, C. N., Zadrazil, I. & Hewit, G. F. Characteristics of horizontal liquid-liquid flows in a circular pipe using simultaneous high-speed laser-induced fluorescence and particle velocimetry. *Int. J. Multiphase Flow* **49**, 99–118 (2013).
5. Gao, Z.-K., Zhang, X.-W., Jin, N.-D., Marwan, N. & Kurths, J. Multivariate recurrence network analysis for characterizing horizontal oil-water two-phase flow. *Phys. Rev. E* **88**, 032910 (2013).
6. Jana, A.-K., Das, G. & Das, P.-K. Flow regime identification of two-phase liquid-liquid upflow through vertical pipe. *Chem. Eng. Sci.* **6**, 1500–1515 (2006).
7. Rodriguez, I.-H. *et al.* Drag reduction phenomenon in viscous oil-water dispersed pipe flow: Experimental investigation and phenomenological modeling. *AIChE J.* **58**, 2900–2910 (2012).
8. Chakrabarti, D.-P., Das, G. & Das, P.-K. Identification of stratified liquid-liquid flow through horizontal pipes by a non-intrusive optical probe. *Chem. Eng. Sci.* **62**, 1861–1876 (2007).
9. Angeli, P. & Hewitt, G.-F. Flow structure in horizontal oil-water flow. *Int. J. Multiphase flow* **26**, 1117–1140 (2000).
10. Zhai, L.-S., Jin, N.-D. & Gao, Z.-K. Cross-correlation velocity measurement of horizontal oil-water two-phase flow by using parallel-wire capacitance probe. *Exp. Therm. Fluid Sci.* **53**, 277–289 (2014).
11. Gao, Z.-K., Jin, N.-D., Wang, W.-X. & Lai, Y.-C. Phase characterization of experimental gas-liquid two-phase flows. *Phys. Lett. A* **374**, 4014–4017 (2010).
12. Barabási, A.-L. Scale-free networks: A decade and beyond. *Science* **325**, 412–413 (2009).
13. Vespignani, A. Complex networks: The fragility of interdependency. *Nature* **464**, 984–985 (2010).
14. Newman, M. E. J. *Networks an introduction* (Oxford University Press, 2010).
15. Zhou, S. & Mondragón, R.-J. Structural constraints in complex networks. *New J. Phys.* **9**, 173 (2007).
16. Arenas, A., Diaz-Guilera, A., Kurths, J., Moreno, Y. & Zhou, C. Synchronization in complex networks. *Phys. Rep.* **469**, 93–153 (2008).
17. Stepanenko, A. S., Constantinou, C. C., Yurkevich, I. V. & Lerner, I. V. Temporal correlations of local network losses. *Phys. Rev. E* **77**, 046115 (2008).
18. Serrano, M. A., Krioukov, D. & Boguna, M. Self-similarity of complex networks and hidden metric spaces. *Phys. Rev. Lett.* **100**, 078701 (2008).
19. Huang, Z., Zhang, J., Dong, J., Huang, L. & Lai, Y.-C. Emergence of grouping in multi-resource minority game dynamics. *Sci. Rep.* **2**, 703 (2012).
20. Bagrow, J. P. & Brockmann, D. Natural emergence of clusters and bursts in network evolution. *Phys. Rev. X* **3**, 021016 (2013).
21. Bianconi, G. Statistical mechanics of multiplex networks: Entropy and overlap. *Phys. Rev. E* **87**, 062806 (2013).
22. Wang, Z. *et al.* Impact of social punishment on cooperative behavior in complex networks. *Sci. Rep.* **3**, 3055 (2013).
23. Brockmann, D. & Helbing, D. The hidden geometry of complex, network-driven contagion phenomena. *Science* **342**, 1337–1342 (2013).
24. Lu, J. Q., Ho, D. W. C., Cao, J. D. & Kurths, J. Single impulsive controller for globally exponential synchronization of dynamical networks, Nonlinear Anal.-*Real* **14**, 581 (2013).
25. Caldarelli, G., Chessa, A., Gabrielli, A., Pammolli, F. & Puliga, M. Reconstructing a credit network. *Nature Physics* **9**, 125–126 (2013).
26. Vijayaraghavan, V. S., Noel, P. A., Waagen, A. & D'Souza, R. M. Growth dominates choice in network percolation. *Phys. Rev. E* **88**, 032141 (2013).
27. Molkenthin, N., Rehfeld, K., Marwan, N. & Kurths, J. Networks from flows - from dynamics to topology. *Sci. Rep.* **4**, 4119 (2014).
28. Jin, Q., Wang, L., Xia, C. & Wang, Z. Spontaneous symmetry breaking in interdependent networked game. *Sci. Rep.* **4**, 4095 (2014).
29. Tan, S. & Lu, J. Characterizing the effect of population heterogeneity on evolutionary dynamics on complex networks. *Sci. Rep.* **4**, 5034 (2014).
30. Shen, Z. S., Wang, W. X., Fan, Y., Di, Z. R. & Lai, Y. C. Reconstructing propagation networks with natural diversity and identifying hidden sources. *Nat. Commun.* **5**, 4323 (2014).
31. Fortunato, S. Community detection in graphs. *Phys. Rep.* **486**, 75–174 (2010).
32. Chauhan, S., Girvan, M. & Ott, E. Spectral properties of networks with community structure. *Phys. Rev. E* **80**, 056114 (2009).
33. Newman, M. E. J. & Girvan, M. Finding and evaluating community structure in networks. *Phys. Rev. E* **69**, 026113 (2004).
34. Duch, J. & Arenas, A. Community detection in complex networks using extremal optimization. *Phys. Rev. E* **72**, 027104 (2005).
35. Reichardt, J. & Bornholdt, S. Statistical mechanics of community detection. *Phys. Rev. E* **74**, 016110 (2006).
36. Liu, W., Pellegrini, M. & Wang, X.-F. Detecting communities based on network topology. *Sci. Rep.* **4**, 5739 (2014).
37. Arenas, A., Fernández, A. & Gómez, S. Analysis of the structure of complex networks at different resolution levels. *New J. Phys.* **10**, 053039 (2008).
38. Zhang, J. & Small, M. Complex network from pseudoperiodic time series: topology versus dynamics. *Phys. Rev. Lett.* **96**, 238701 (2006).
39. Lacasa, L., Luque, B., Ballesteros, F., Luque, J. & Nuno, J.-C. From time series to complex networks: The visibility graph. *Proc. Natl. Acad. Sci. USA* **105**, 4972–4975 (2008).
40. Xu, X., Zhang, J. & Small, M. Superfamily phenomena and motifs of networks induced from time series. *Proc. Natl. Acad. Sci. USA* **105**, 19601–19605 (2008).
41. Li, X., Yang, D., Liu, X. & Wu, X. M. Bridging time series dynamics and complex network theory with application to electrocardiogram analysis, IEEE circuits and systems magazine, **12**, 33–46 (2012).
42. Gao, Z.-K. & Jin, N.-D. A directed weighted complex network for characterizing chaotic dynamics from time series. *Nonlinear Analysis-Real World Applications* **13**, 947–952 (2012).
43. Donges, J.-F., Heitzig, J., Donner, R.-V. & Kurths, J. Analytical framework for recurrence network analysis of time series. *Phys. Rev. E* **85**, 046105 (2012).
44. Huang, L., Lai, Y.-C. & Harrison, M. A. F. Probing complex networks from measured time series. *Int. J. Bifurcat. Chaos* **22**, 1250236 (2012).
45. Iwayama, K. *et al.* Characterizing global evolutions of complex systems via intermediate network representations. *Sci. Rep.* **2**, 423 (2012).
46. Donges, J.-F. *et al.* Nonlinear detection of paleoclimate-variability transitions possibly related to human evolution. *Proc. Natl. Acad. Sci. USA* **108**, 20422–20427 (2011).
47. Steinhaeuser, K., Ganguly, A. R. & Chawla, N. V. Multivariate and multiscale dependence in the global climate system revealed through complex networks. *Climate Dynamics* **39**, 889–895 (2012).
48. Hempel, S., Koseska, A., Kurths, J. & Nikoloski, Z. Inner composition alignment for inferring directed networks from short time series. *Phys. Rev. Lett.* **107**, 054101 (2011).
49. Chavez, M., Valencia, M., Navarro, V., Latora, V. & Martinerie, J. Functional modularity of background activities in normal and epileptic brain networks. *Phys. Rev. Lett.* **104**, 118701 (2010).
50. Walker, D.-M., Tordesillas, A., Nakamura, T. & Tanizawa, T. Directed network topologies of smart grain sensors. *Phys. Rev. E* **87**, 032203 (2013).
51. Wang, W.-X., Yang, R., Lai, Y.-C., Kovanis, V. & Grebogi, C. Predicting catastrophes in nonlinear dynamical systems by compressive sensing. *Phys. Rev. Lett.* **106**, 154101 (2011).
52. Ghaffari, H.-O. & Young, R.-P. Acoustic-friction networks and the evolution of precursor rupture fronts in laboratory earthquakes. *Sci. Rep.* **3**, 1799 (2013).

53. Tang, J.-J., Wang, Y.-H., Wang, H., Zhang, S. & Liu, F. Dynamic analysis of traffic time series at different temporal scales: A complex networks approach. *Physica A* **405**, 303–315 (2014).
54. Charakopoulos, A., Karakasidis, T.-E., Papanicolaou, P.-N. & Liakopoulos, A. The application of complex network time series analysis in turbulent heated jets. *Chaos* **24**, 024408 (2014).
55. Gao, Z.-K. & Jin, N.-D. Flow-pattern identification and nonlinear dynamics of gas-liquid two-phase flow in complex networks. *Phys. Rev. E* **79**, 066303 (2009).
56. Gao, Z.-K., Jin, N.-D., Wang, W.-X. & Lai, Y.-C. Motif distributions in phase-space networks for characterizing experimental two-phase flow patterns with chaotic features. *Phys. Rev. E* **82**, 016210 (2010).
57. Gao, Z.-K. *et al*. Recurrence networks from multivariate signals for uncovering dynamic transitions of horizontal oil-water stratified flows. *Europhys. Lett.* **103**, 50004 (2013).
58. Gao, Z.-K. *et al*. Recurrence network analysis of experimental signals from bubbly oil-in-water flows. *Phys. Lett. A* **377**, 457–462 (2013).
59. Gao, Z.-K., Fang, P. C., Ding, M. S. & Jin, N.-D. Multivariate weighted complex network analysis for characterizing nonlinear dynamic behavior in two-phase flow. *Experimental Thermal and Fluid Science* **60**, 157–164 (2015).
60. Watts, D.-J. & Strogatz, S.-H. Collective dynamics of 'small-world' networks. *Nature* **393**, 440–442 (1998).

Acknowledgments

Z. K. Gao was supported by National Natural Science Foundation of China under Grant Nos. 61473203 and 61104148, Specialized Research Fund for the Doctoral Program of Higher Education of China under Grant No. 20110032120088, Elite Scholar Program of Tianjin University. N. D. Jin was supported by National Natural Science Foundation of China under Grant No. 41174109, and National Science and Technology Major Project of China under Grant No. 2011ZX05020-006. C. Y. Xia was supported by National Natural Science Foundation of China under Grant No. 61374169.

Author contributions

Z.K.G. and N.D.J. devised the research project. Z.K.G., N.D.J., P.C.F. and L.D.H. conducted the experiment. Z.K.G., Y.X.Y., P.C.F. and L.D.H. performed numerical simulations. Z.K.G., Y.X.Y., N.D.J. and C.Y.X. analyzed the results and wrote the paper.

Additional information

Competing financial interests: The authors declare no competing financial interests.

How to cite this article: Gao, Z.-K. *et al*. Multi-frequency complex network from time series for uncovering oil-water flow structure. *Sci. Rep.* **5**, 8222; DOI:10.1038/srep08222 (2015).